



## A reanalysis of one decade of the mass balance series on Hintereisferner, Ötztal Alps, Austria: a detailed view into annual geodetic and glaciological observations

Christoph Klug<sup>1</sup>, Erik Bollmann<sup>1</sup>, Stephan P. Galos<sup>2</sup>, Lindsey Nicholson<sup>2</sup>, Rainer Prinz<sup>3</sup>, Lorenzo Rieg<sup>1</sup>,  
5 Rudolf Sailer<sup>1</sup>, Johann Stötter<sup>1</sup> and Georg Kaser<sup>2</sup>

<sup>1</sup> Institute of Geography, University of Innsbruck, Austria

<sup>2</sup> Institute of Atmospheric and Cryospheric Sciences, University of Innsbruck, Austria

<sup>3</sup> Department of Geography and Regional Science, University of Graz, Austria

10

Correspondence to: Christoph Klug ([Christoph.klug@uibk.ac.at](mailto:Christoph.klug@uibk.ac.at))

**Abstract.** This study presents a reanalysis of the glaciologically obtained 2001–11 annual glacier mass balances record at  
15 Hintereisferner, Ötztal Alps, Austria. The reanalysis is accomplished through a comparison with geodetically derived mass  
changes, using annual high-resolution airborne laser scanning (ALS). The grid based adjustments for the method-inherent  
differences are discussed along with associated uncertainties and discrepancies of the two forms of mass balance  
measurements. A statistical comparison of the two datasets shows no significant difference for seven annual as well as the  
20 cumulative mass changes over the ten years record. Yet, the statistical view hides significant differences in the mass balance  
years 2002/03 (glaciological minus geodetic records = +0.92 m w.e.), 2005/06 (+0.60 m w.e.) and 2006/07 (−0.45 m w.e.).  
The validity of the results is critically assessed and concludes that exceptional atmospheric circumstances can render the  
usual glaciological observational network inadequate. Furthermore, we consider that ALS data reliably reproduce the annual  
mass balance and can be seen as calibration tools of or, under certain circumstances, even as a substitute for the glaciological  
method.

### 25 1 Introduction

The mass balance of a glacier defines its hydrological reservoir function (e.g. Kaser et al., 2010) and is a high-confidence  
indicator of climate change (e.g. Vaughan et al., 2013; Bojinski et al., 2014). There are two primary methods for determining  
the mass balance of a glacier. The glaciological method is the most widely used for assessing annual and – more rarely –  
seasonal mass changes of individual glaciers (e.g. Anonymous, 1969; Hoinkes, 1970; Kaser et al., 2003; Cogley et al., 2011).  
30 It spatially extrapolates in situ point measurements of ablation and accumulation to the glacier-wide surface mass balance,  
encompassing changes at the glacier surface (Cogley et al., 2011). Earliest glacier mass balance measurements started around  
1950, but only about 30 reference glaciers have uninterrupted annual time series going back to 1976 (e.g. Zemp et al. 2009).  
This small number of annually measured glacier mass balance series provides the basis for reconstructing past contributions



to sea level rise (e.g. Kaser et al., 2006; Marzeion et al., 2012; Gardner et al., 2013; Vaughan et al., 2013), extrapolating  
35 glaciers' contribution to regional water supply (e.g. Kaser et al., 2010, Weber et al., 2010, Huss, 2011, Bliss et al. 2014), and  
glacier change detection, attribution (Marzeion et al., 2014; Slangen et al., 2016) and projection studies (e.g. Radić and  
Hock, 2006; Marzeion et al., 2012; Radić et al., 2013; Huss and Hock, 2015; Mengel et al., 2016).

The surface mass balance is defined as the mass change at the glacier surface and within the snow cover which evolves  
during the balance year (cf. Cogley et al. 2011). In contrast to the surface mass balance obtained with the glaciological  
40 method, the geodetic method subtracts two consecutive digital terrain models (DTMs) of a glacier and provides its volume  
change. This method integrates over all processes that lead to surface height changes at any single point of a glacier, i.e. the  
surface, internal, and basal mass changes as well as those from ice flux divergence, and densification (Cuffey and Paterson,  
2010). Consequently, the mass balance values at a certain point of the glacier may differ significantly between the  
glaciological and the geodetic mass balance method. However, according to the principals of mass conservation, the ice flux  
45 divergence becomes zero if integrated over an entire glacier. Moreover, by assuming internal and basal mass changes on mid  
latitude mountain glaciers to be of minor importance (e.g. Cuffey and Paterson, 2010), and by applying either measured or  
estimated snow or ice density to convert volume into mass changes, the two methods should obtain fairly similar numbers  
for the total mass balance. In this way, geodetically obtained results have been used as controls for annual glaciological mass  
balances at decadal scales and are commonly applied to identify random and to correct systematic uncertainties in  
50 glaciological mass balance time series (Hoinkes, 1970; Haeberli, 1998; Fountain et al., 1999; Krimmel, 1999; Østrem and  
Haakensen, 1999; Hagg et al. 2004; Cox and March, 2004, Huss et al., 2009; Thibert and Vincent, 2009; Koblet et al., 2010;  
Zemp et al., 2010; Prinz et al., 2011; Zemp et al., 2013; Galos et al., 2017). Geodetic measurements have also been merged  
with glaciological mass balance series to increase coverage and representativeness of large regions' and global glacier mass  
balance information (e.g. Cogley 2009; Gardner et al., 2013). Indeed, the interconnection of different methods is increasingly  
55 suggested in order to ensure progress in glacier mass change estimates for large regions or even on the global scale (Gardner  
et al., 2013; Marzeion et al., 2017).

At Hintereisferner in the Austrian Ötztal Alps, glaciological and photogrammetry based geodetic mass balances are available  
since the early 1950s (e.g. Kuhn et al., 1999). Early analyses showed good agreement between the two data series on a  
decadal time scale for the periods 1952/53 to 1963/64 (Lang and Patzelt, 1971) and 1952/53 to 1990/91 (Kuhn et al., 1999).  
60 Yet, a more detailed examination by Zemp et al. (2013) revealed discrepancies at Hintereisferner for the periods 1963/64 to  
1968/69 and 1978/79 to 1990/91.

Geodetic mass balances for Hintereisferner were obtained at annual time steps between 2001 and 2011, when high resolution  
air borne laser scanning (ALS) became available. Gross results from the first data pairs indicated considerable differences to  
the glaciological mass balances (Geist and Stötter, 2007). These differences and the meanwhile available 11 annual high-  
65 quality ALS-data sets motivate and enable a so far unique validation and, finally, a reanalysis of annual surface mass  
balances of a glacier.



This study presents the first use of annual geodetic records for a detailed reanalysis of an annual glaciological mass balance record. This is achieved by a stepwise assessment of method-inherent uncertainties in each dataset ( $\sigma$ ; section 3) and the accounting for method-inherent differences ( $\epsilon$ ) between the surface (glaciological) and the total (geodetic) mass balance  
70 (section 4). In section 5 we thoroughly perform and discuss the final reanalysis of the glaciological record, ending with concluding remarks in section 6.

## 2 Hintereisferner

Hintereisferner (46.79°N, 10.74°E) is a valley glacier in the Austrian part of the Ötztal Alps (Figure 1). The glacier consists of three main tributary basins. Langtaufereerjochferner (1.11 km<sup>2</sup>) and Stationsferner (0.28 km<sup>2</sup>) disconnected from  
75 Hintereisferner in 1969 and 2000, respectively, but are still treated as part of the glacier in mass balance assessments in order to maintain consistency over the whole time series of observations. Hence, “Hintereisferner” in this paper refers to all three glacier bodies.

The area of Hintereisferner in 2011 was 6.78 km<sup>2</sup>, about 15% smaller than in 2001, when the first ALS campaign was conducted. The glacier front retreated by 390 m during the same period. The glacier elevation ranges from 2456 to 3720 m  
80 a.s.l. and the median altitude is 3039 m a.s.l. The accumulation area covers aspects from northeast to southeast while the long and narrow tongue faces northeast. Meltwaters feed the Hintereisbach, which joins the runoff from Kesselwandferner, Hochjochferner and a few smaller glaciers and subsequently drains into Rofenache and finally into the Ötztaler Ache, one of the major tributaries of the Inn River.

Hintereisferner is located in the ‘inner dry Alpine zone’ (Frei and Schär, 1998), which is amongst the driest regions of the  
85 entire European Alps. Precipitation in Vent (~1900 m a.s.l.), about 8 km west of the glacier terminus, reaches 677 mm a<sup>-1</sup>, with air temperatures of 1.5°C in average (1906–2011). Precipitation amounts double at the totalizing rain gauge near the Hintereis research station (3026 m a.s.l.; Figure 1), reflecting the altitudinal difference of approximately 1100 m but also the enhanced precipitation activity further up the valley. Over the study period 2001 to 2011, the values for annual temperature and precipitation in Vent are 2.3°C and 676 mm, respectively. The mean annual 0°C-isotherm is located at ~ 2450 m a.s.l.

90 Like many glaciers in the Eastern European Alps, Hintereisferner has experienced strong shrinkage compared to its Little Ice Age maximum extent, which was reached sometime between 1847 and 1855 (Richter, 1888). Since that time, the glacier area in the Ötztal-Alps has shrunk by more than 50% (Fischer et al. 2015). After a period of rather stationary glacier lengths in the late 1970s and early 1980s (e.g. Patzelt, 1985), glacier mass loss and area shrinkage dominate with particularly high rates during and after the extraordinarily hot summer of 2003 (e.g. Abermann et al., 2009).



### 95 3 Mass balance methods and data

In this section we introduce the glaciological and the geodetic measurement methods used to obtain the annual mass balances of Hintereisferner. We first determine a common base for the two datasets, by the homogenization of glacier outlines and DTMs, followed by quantifying method-inherent uncertainties.

#### 3.1 The glaciological method

100 Glaciological measurements of annual mass balance at Hintereisferner have been started in 1952 (Hoinkes, 1970) and are carried out regularly since then, resulting in one of the longest continuous glacier mass balance time series worldwide. The distribution of 40 to 50 (maximum 100) ablation stakes over the main tongue of Hintereisferner is a compromise between representative coverage and logistic feasibility (Kuhn et al, 1998; Fischer, 2009). During the study period no ablation stakes are placed in the upper part of the glacier, where the accumulation is usually determined by means of snow pits and probings  
105 at the end of the mass balance year. The location of individual snow pits has been more or less constant over the whole study period. Their number changed according to the varying extent of the accumulation area from none in e.g. 2002/03 up to 14 pits in 2003/04 (see Figure 1). The series follows the fixed date system as defined by the hydrological year, spanning from October 1st to September 30th of the following year, with additional measurements in spring and during about fortnightly visits between June and October.

110 The annual mass balance at each measurement point is derived by converting the individual change of surface height as obtained from stakes and pits. Ice ablation obtained from repeat stake readings is converted into point specific mass balance by applying an assumed constant density of 900 kg m<sup>-3</sup>. Accumulation is determined by measuring the snow depth in conjunction with depth-averaged snow density in snow pits. The point values and additional observational information such as the position of the snowline from an automatic camera and from terrestrial and air photographs, topographic conditions,  
115 and the expert knowledge about typical spatial patterns are the basis for drawing contour lines of equal mass balance values. The resulting areas of equal mean mass balance are then intersected with 50 m altitude bands in order to derive the vertical mass balance profile. By integrating over the altitude bands, both the total mass balance  $B_{glac}$  and the mean specific mass balance of the entire glacier  $b_{glac}$  are obtained (e.g. Kaser et al., 2003; Cogley et al., 2011). Results are submitted to the World Glacier Monitoring Service (WGMS) annually. In order to provide a common base for both the glaciological and  
120 geodetic analyses we re-generate the annual glacier outlines from the ALS data rigorously following the guidelines presented in Abermann et al. (2010). This led to minor changes ( $\epsilon_{area}$ ) in annual glaciological balances in the order of  $-0.015$  to  $+0.039$  m w.e. a<sup>-1</sup>, accumulating to  $+0.12$  m w.e. over the 2001 to 2011 period.

Before approaching the reanalysis of the annual surface mass balances of Hintereisferner for the time period 2001 to 2011  
125 further uncertainties in the glaciological mass balances series must be addressed. The glaciological method suffers from uncertainties related to (i) point measurements and (ii) their spatial extrapolation over the entire glacier. For both uncertainty



sources and due to the lack of respective data on Hintereisferner we synthesize appropriate information from the literature as follows.

130 Zemp et al. (2013) analysed, among others, the mass balance series of Hintereisferner for six periods between 1953 and 2006 and attributed an uncertainty of  $\pm 0.10$  m w.e.  $a^{-1}$  to field measurements for the years after 1964 and doubled the value for the years before. For the spatial interpolation of point data they assigned values between  $\pm 0.14$  and  $\pm 0.54$  m w.e.  $a^{-1}$  with an average of  $\pm 0.33$  m w.e.  $a^{-1}$  for the entire period. Further explanations are not provided by Zemp et al. (2013).

135 Fountain and Vecchia (1999) found combined uncertainties for (i) and (ii) of up to  $\pm 0.33$  m w.e.  $a^{-1}$  by analysing the modelled variability of the mass balance of South Cascade glacier. Thibert et al. (2008) and Thibert and Vincent (2009) analysed 51 years of mass balance for Glacier de Sarennes and reported a combined annual uncertainty of  $\pm 0.20$  m w.e.  $a^{-1}$  for (i) and (ii). For Gries- and Silvrettagletscher, Huss et al. (2009) assumed overall uncertainties related to (i) and (ii) of  $\pm 0.16$  to  $\pm 0.28$  m w.e.  $a^{-1}$ . By investigating the glaciological and geodetic mass balances of Storglaciären, Zemp et al. (2010) determined the random uncertainty for (i) and (ii) with  $\pm 0.10$  m w.e.  $a^{-1}$  each, which resembles the results of Jansson (1999). For Findelengletscher, Sold et al. (2016) roughly estimated a random uncertainty of  $\pm 0.04$  m w.e.  $a^{-1}$  for (i), referring to Huss et al. (2009), and of  $\pm 0.17$  m w.e.  $a^{-1}$  for (ii) by evaluating contour lines drawn by 18 independent analysers. On Nigardsbreen, Andreassen et al. (2016) obtained a total point measurement uncertainty of  $\pm 0.25$  m w.e.  $a^{-1}$  as the root sum square (RSS) of a false determination of the previous year's summer surface ( $\pm 0.15$  m w.e.  $a^{-1}$ ), upwelling of stakes ( $\pm 0.20$  m w.e.  $a^{-1}$ ), and wrong density assumptions of snow and firn ( $\pm 0.05$  m w.e.  $a^{-1}$ ). Uncertainty of spatial integration was taken as  $\pm 0.21$  m w.e.  $a^{-1}$ , made up by point measurements insufficiently covering both the vertical range and the total area of  
145 the glacier.

Based on the findings of Zemp et al. (2013) combined with expert knowledge about the study site, we assess the uncertainty related to point measurements at Hintereisferner, being in the order of  $\sigma_{\text{point}} = \pm 0.10$  m w.e.  $a^{-1}$ , resulting in a decadal value of about  $\pm 0.32$  m w.e. For extrapolating point data into reasonable patterns of mass balance, the contour line method uses expert knowledge. Based on Sold et al. (2016), we estimate a respective uncertainty of  $\pm 0.15$  m w.e.  $a^{-1}$  for Hintereisferner.  
150 In addition and according to Andreassen et al. (2016), we assume that the extrapolation over areas not covered by point measurements inherits uncertainties of  $\pm 0.10$  m w.e.  $a^{-1}$ . Hence, uncertainty due to spatial integration of the respective measurements over the entire glacier is defined to be  $\sigma_{\text{spatial}} = \pm 0.18$  m w.e.  $a^{-1}$  and result in decadal uncertainty of  $\pm 0.57$  m w.e.

Overall uncertainties for the glaciological mass balances are calculated, according to the law of error propagation, leading to  
155  $\sigma_{\text{glac}} = \pm 0.21$  m w.e. for annual and  $\pm 0.65$  m w.e. for the cumulated values.

### 3.2 The geodetic method

Between 2001 and 2011, eleven ALS flight campaigns had been carried out near the end of each mass balance year (see Table 1). During each ALS data acquisition campaign, the glacier was covered with a number of overlapping flight strips in



order to increase the point density and to ensure high quality and complete coverage of the glacier (Wever and Lindenberger  
160 1999; Geist and Stötter, 2007).

As there is essentially no high vegetation in the study area, ALS points are classified into ground points and flying objects  
(outliers) only. The ground points of all datasets are imported into a laser database system (Rieg et al., 2014) which  
facilitates storage and further processing. 1 m resolution DTMs are calculated for all datasets, whereby the mean value of all  
ALS points located in each cell represents the elevation of the cell. The elevation values for the few raster cells that do not  
165 contain a single point are interpolated from the neighbouring cells using a least squares method.

In order to provide high-quality DTMs used for mass balance calculations, horizontal misalignment of the DTMs being  
differenced has to be excluded. Therefore a statistical co-registration correction procedure as suggested by Nuth and Kääb  
(2011) was performed for this study. Following Joerg et al. (2012) we applied the first two steps of the procedure to the ice-  
free areas for identifying potential horizontal shifts and vertical offsets between two ALS-DTMs. The statistical co-  
170 registration reveals horizontal shifts smaller than the DTM pixel resolution with no elevation-dependent bias, and the DTMs  
can be subtracted from each other without performing DTM corrections.

The total volume change  $\Delta V$  between two dates is then derived from the respective elevation difference  $\Delta h_k$  of the two grids  
at pixel  $k$  with cell size  $r$  of the DTMs, summed over the number of pixels  $k$  covering the glacier at the maximum extent and  
is expressed as (cf. Zemp et al., 2013):

175

$$\Delta V = r^2 \sum_{k=1}^K \Delta h_k, \quad (1)$$

For a comparison with the glaciological balance,  $\Delta V$  is then converted into a specific mass balance in the unit metre water  
equivalent (m w.e.):

180

$$B_{geod} = \frac{\Delta V}{S_{t1}} \times \frac{\bar{\rho}}{\rho_{water}}, \quad (2)$$

where  $\frac{\bar{\rho}}{\rho_{water}}$  is the ratio between the average bulk density of  $\Delta V$  and the density of water,  $t_1$  referring to the first acquisition  
date.

185 Despite a thorough co-registration, surface elevation differencing of two DTMs is still subject to various uncertainties. The  
vertical accuracy of the raw ALS point data was first assessed by comparing the point clouds with differential global  
navigation satellite system (dGNSS) measured points on a homogeneous horizontal surface outside the study area (e.g. in our  
case a football field in Zwieselstein 20 km down-valley of Hintereisferner). Table 1 shows the standard deviations (SD) of  
vertical accuracies of the individual datasets.



190 As the reference surface does not reflect the surface conditions in terms of slope, aspect and roughness, and therefore is not  
representative for vertical accuracies, Bollmann et al. (2011) compared dGNSS ground control points with laser returns  
(deviation to laser points 0.07 m, standard deviation 0.08 m) and calculated an absolute slope-dependent vertical accuracy  
for Hintereisferner ALS point data (<0.10 m on slopes <40°). Sailer et al. (2014) analysed the uncertainties resulting from  
rasterizing laser point clouds, revealing that a cell size of 1x1 m as used for our study causes only negligible errors of less  
195 than 0.10 m.

For the raw geodetic balance ( $b_{\text{geod,raw}}$ ), the results of DTM differencing over stable terrain are taken to define uncertainties  
associated with the DTM comparison. Therefore, we selected five stable control areas ( $\sim 3 \times 10^4 \text{ m}^2$ ) surrounding the glacier  
(Figure 1), in order to quantify grid-based uncertainties of spatially averaged elevation differences. As the standard deviation  
of the elevation differences ( $SD\Delta z$ , Table 2) provides information on the spatial variability of the selected stable areas, we  
200 used the related RSS for an approximation to our DTM uncertainty:

$$\sigma_{DTM} = \sqrt{\sum_1^i SD_i^2}, \quad (3)$$

where SD is the standard deviation within the reference surfaces  $i$ . The result was converted into mass using the density of  
ice. Comparison of the differential DTMs (dDTMs) show uncertainties of  $\pm 0.06 < \sigma_{DTM} < \pm 0.17 \text{ m w.e.}$ , resulting in  
205  $\pm 0.36 \text{ m w.e.}$  cumulated over the observation period (01-11cum; Table 3). In contrast, the 2001 to 2011 one step application  
of the geodetic method (01/11; Table 3) yields a value of  $\sigma_{DTM} = \pm 0.14 \text{ m w.e.}$

Table 3 summarizes the results of sections 3.1 and 3.2 and shows the differences between the adjusted glaciological and the  
raw geodetic mass balances ( $b_{\text{glac,hom}} - b_{\text{geod,raw}}$ ).

210

#### 4 Accounting for method inherent differences

Figure 2 shows the glaciological and the geodetic mass balance series as revised in sections 3.1 and 3.2. The expected  
differences vary from year to year, being particularly high in some years (Table 3). The potential causes of these  
discrepancies in the mass balance series are related to snow cover at the time of ALS acquisition (4.1), different glacier-wide  
215 density assumptions in mass balance calculation (4.2), survey date differences between the glaciological and geodetic  
observations (4.3), the way the methods consider the existence of crevasses (4.4), and the differences between the surface  
(glaciological) and the total (geodetic) mass balance (4.5).



#### 4.1 Differences induced by snow cover present in DTMs

Whereas the vertical accuracy tends to be very high, biases as a result of snowfall events preceding the ALS surveys  
220 influence the calculated volume change significantly. From the analysis of elevation differences in the non-glaciated terrain,  
the mean difference between two DTMs ( $\overline{\Delta z}$  stable areas; Table 2) with

$$\varepsilon_{DTM} = \frac{\sum_1^n \overline{\Delta z}_t}{n}, \quad (4)$$

225 where  $n$  is the number of DTM grid cells covering non-glacierized terrain, can be used for inevitable volume corrections,  
caused by preceding snow fall events.

For the periods 2001/02, 2005/06, 2006/07 and 2007/08 the investigation of stable areas within the dDTMs revealed snow  
induced vertical offsets between  $|0.18|$  and  $|0.58|$  m ( $\overline{\Delta z}$ ; bold numbers in Table 3). In all other dDTMs, the vertical bias was  
below 0.10 m. In 2004 and 2010 a snow fall event occurred some days before the ALS measurements. However, this is not  
230 reflected in the stable areas of the respective dDTM, because the snow in non glacierized areas had melted from off-glacier  
surface by the time of the ALS survey. This leads to a very low offset in the non-glacierized terrain in the related mass  
balance periods. Yet, as snow cover increases, the ALS elevations measured on reference surfaces have to be cross-checked  
with the closest field survey data for snow depth estimation and subsequently corrected. Based on the altitude distribution of  
stable areas and in-situ measurements a linear regression in 50 m elevation bands yielded mean snow depths of 0.52 m in  
235 2001, 0.23 m in 2004, 0.46 m in 2005, 0.13 m in 2006, 0.12 m in 2007 and 0.26 m in 2010. This leads to adjusted DTMs  
and, finally, to a respective mass balance correction value  $\varepsilon_{DTM}$  (Table 5). Furthermore this approach was integrated to the  
estimation of differences related to unequal survey dates (see section 4.3)..

#### 4.2 Density conversion

240 One of the method-inherent differences between glaciological and geodetic method can be found in the density conversion.  
Glaciological mass balances are derived from mass change measurements based on well constrained in situ density  
measurements, whereas the geodetic ones are based on volume change measurements, which require conversion to mass by  
an estimated density for the material lost or gained (e.g. Thomson et al., 2016). Several studies assume that density in the  
accumulation area is constant over time and, hence, use glacier ice density for the conversion (e.g. Andreassen, 1999; Haug  
245 et al., 2009). As long as snow or firn is present, the density of ice ( $\rho_{ice}=900 \text{ kg m}^{-3}$ ) causes an overestimation of the mass  
change. Hence, only below the equilibrium line altitude (ELA), where altitudinal changes are either due to ice ablation or  
emergence, the density of ice is appropriate. However, if firn line changes are known, the volume to mass conversion can be  
approximated by an average density of firn (e.g. Sapiano et al., 1998; Prinz et al., 2011). To make a first calculation of mass  
change (Figure 2), we follow the recommended approximation for density conversion of  $850 \pm 60 \text{ kg m}^{-3}$  suggested by Huss



250 (2013). However, this approach revealed differences in some periods of the data series, as the assumption of Huss (2013) is suitable for geodetic analyses over periods which span over five years or more and which show relatively stable mass balance gradients, non-negligible changes in volume and a relatively stable extent of the firn region.

Therefore we designed a pixel-based surface classification workflow, in order to account for changing firn areas. The present classification is based on ALS-intensity data as described by Höfle and Pfeifer (2007). Following Fritzmann et al. (2011), a classification of ice and firn zones on the glacier surface for each survey year could be achieved (Figure 3).

265 If no suitable intensity data are available from the ALS, the most contemporary ortho-images (e.g. for the year 2010) and/or LandsatTM images (e.g. for the years 2001 and 2004) are used for surface classification. To incorporate the changing extent of the perennial firn zones we subtracted the surface grids of the respective mass balance periods from each other and reclassified the resulting new surface raster. The glacier surface is classified in two categories: glacier ice with a density of  
260  $900 \pm 17 \text{ kg m}^{-3}$  and perennial firn with  $700 \pm 50 \text{ kg m}^{-3}$  (Ambach and Eisner, 1966; Huss, 2013), whereas the difference to maximum/minimum estimates ( $\pm 17$  and  $\pm 50 \text{ kg m}^{-3}$ ) serve as an uncertainty measure within our approach ( $\sigma_{\kappa}$ ; Table 5). The resulting grids are used to convert volumetric changes into a mass for every pixel (see equation 2). For a better interpretation we introduce a dimensionless conversion factor as

$$265 \quad \kappa = \frac{\rho_{ice} \cdot \Delta V_{ice} + \rho_{firn} \cdot \Delta V_{firn}}{\rho_{water} \cdot \Delta V_{total}} . \quad (5)$$

Corresponding volume-to-mass conversion factors ( $\kappa$ ) lie in the range of 820 and 930. The change in mass balance values compared to the raw geodetic results (Table 2) is ascribed to the density conversion deviation ( $\epsilon_{\kappa}$ ; Table 5).

#### 4.3 Survey date differences

270 Temporal differences between the geodetic and glaciological observations need to be addressed. To align the geodetic dates with the stratigraphic year used for the glaciological mass balance measurements, a multi-methodical approach was applied, incorporating field measurement minutes, DTM analysis results from section 4.1 and data from in situ measurements.

Apart from 2011 with in situ measurements conducted on the same day as the ALS flight (Table 4), the changes in snow depth and ice ablation between the two measuring dates have to be considered. If the date of the ALS acquisition deviates  
275 from the 30th of September (end of the hydrological year), the geodetic mass balance is adjusted to the fixed dates by linear extrapolations as follows. In case of ablation between the survey and the fixed date the extrapolation is based on the ablation trend over the immediately preceding time for each stake. This is calculated from available stake readings during the summer justified by extrapolated air temperature data from Vent allowing ablation conditions. In the case of accumulation between the survey and the fixed date, the precipitation gradient between Vent and five rain gauges in the Hintereisferner basin  
280 (Figure 1) is used for adjustment to the fixed date. The snow-rain threshold of  $0^{\circ}\text{C}$  is obtained from the Vent temperatures along a lapse rate of  $0.0065^{\circ}\text{K m}^{-1}$ .



The survey date adjustment is performed individually for each annual geodetic mass balance, dependent on the presence/absence of snow during the field survey and ALS data acquisition as well as on the difference between the survey dates and the end of the hydrological mass balance year. Accordingly, we proceeded as follows:

285

- i) If there was no snow cover during both surveys, and the ALS campaign took place before the field survey, an elevation dependent mean ablation gradient as described above is applied. This is the case in 2003 and 2008.
- ii) If there was no snow cover present during the field survey, but before a later ALS campaign, the mass balance has been adjusted to the survey date by subtracting the amount of snow from the corresponding DTM, as described in section 4.1. This is the case for the years 2006 and 2007. The amount of snow determined agrees well for these years with extrapolated precipitation data using the altitudinal gradients between 5 rain gauges in the area.
- iii) If snow was present during the field survey, but the ALS campaign had been conducted before the snowfall event, the mass of the snow cover measured during the field survey is added to the geodetic mass balance using the measured densities and the linear regression of snow probings for the elevation distribution. This is the case in 2002 and 2008.
- iv) If snow was present during the field survey and the ALS data acquisition, the ALS-DTM was adjusted regarding the snow cover conditions. When the ALS campaign was conducted after the field survey, the geodetic determined snow height is subtracted (section 4.1), and the mass of snow determined by field survey is added to the geodetic mass balance. This is the case for the years 2001, 2004, 2005, 2010.

300

There were no cases with snowfall between both surveys when the ALS data have been acquired before the field data. It is noted that two corrections have been applied for the year 2008 when the ALS data acquisition took place 21 days before the field survey and ablation as well as accumulation occurred. No survey date correction was necessary for 2009 and 2011.

#### 4.4 Representation of crevasses

305

While crevasses are neglected in the glaciological method, they are partially resolved in the geodetic method. Although some crevasses might have been covered by snow during data acquisition, in all DTMs a number of big crevasses are visible, which open during the ablation season. However, depending on snow / melt conditions, crevasses are differently represented in the respective dDTMs, due to the ice movement between two ALS acquisitions and therefore have different impacts on mass balance calculations. We detected crevasses by assuming that they are deviations from a regular homogenous surface.

310

By using the variance as a measure of terrain smoothness and applying a closing filter, we derived a surface without crevasses (for detail we refer to Kodde et al., 2007 and Geist and Stötter, 2010). Hence, we calculated the volume change of a “crevasse free” glacier, to quantify differences due to open crevasses in the geodetic mass balance ( $\epsilon_{\text{crev}}$ ; Table 5).



#### 4.5 Internal and basal mass changes

Internal and basal mass balances are not captured by the glaciological method, but are implicitly included in the geodetic  
315 mass balances. Thus, when comparing glaciological with geodetic balances, internal and basal mass changes need to be  
assessed separately. Particularly for mountain glaciers studies on this topic are rare and published values represent estimates  
rather than verified measurements.

On Storglaciären, for example, Östling and Hooke (1986) estimated the contribution of basal melt due to geothermal heat as  
about 0.001 m w.e. a<sup>-1</sup> and Holmlund (1987) suggested 0.01 m w.e. a<sup>-1</sup> of internal melting by released potential energy from  
320 descending water. Albrecht et al. (2000) considered internal ablation due to ice motion being small on Storglaciären and,  
thus, negligible. For South Cascade Glacier, Mayo (1992) estimated the combined effect of either frictional or geothermal  
basal melt, melt by the loss of potential energy of water flowing through the glacier and melt by the loss of potential energy  
of the ice mass as 0.09 m w.e. a<sup>-1</sup>. Thibert et al. (2008) estimated 0.48 m w.e. of basal ablation due to geothermal heat and  
0.42 m w.e. of internal due to water flow on Glacier de Sarennes over a period of 51 years. Huss et al. (2009) estimated the  
325 contribution to ablation from geothermal heat, internal deformation, and basal friction as -0.01 m w.e. a<sup>-1</sup> for glaciers in the  
Alps. Andreassen et al. (2016) calculated internal and basal ablation due to heat of dissipation based on Oerlemans (2013)  
for 10 glaciers in Norway, yielding a range of 0.01 to 0.08 m w.e. a<sup>-1</sup>. Sold et al. (2016) assessed a value of 0.014 m w.e. a<sup>-1</sup>  
for internal and basal processes at Findelengletscher following different previous studies (e.g. Herron and Langway, 1980;  
Pfeffer et al., 1991; Medici and Rybach, 1995; Huss, 2013).

330 In this study, we assess internal and basal ablation due heat of dissipation following Oerlemans (2013) and Andreassen et al.  
(2016), because it is the most appropriate method for the available data for Hintereisferner. The methodical disregard of  
internal and basal processes in the glaciological mass balance ( $\epsilon_{\text{int}}$ ; Table 5) is assumed to yield values of internal ablation  
around -0.04 m w.e. a<sup>-1</sup>, which corresponds well to published data in Oerlemans (2013) for glaciers of the size and climate  
setting like Hintereisferner. According to Huss et al. (2009) melt from basal friction and geothermal heat flux was estimated  
335 about -0.01 m w.e. a<sup>-1</sup> (hence, -0.05 m w.e. a<sup>-1</sup> cumulated). As the uncertainty of internal and basal processes was not  
subject to any detailed analyses due to lack of independent data, we assume a value of our estimation of  $\pm 30\%$  or  $\pm 0.015$  m  
w.e. a<sup>-1</sup> ( $\sigma_{\text{int}}$ ; Table 5).

#### 5 Reanalysing the glaciological records

The geodetic balance over the entire study period was mainly affected by snow being present in the year 2001 resulting in  
340  $\epsilon_{\text{DTM}} = +0.29$  m w.e. Taking snow heights and densities in DTMs of individual years into account leads to  $-0.41 < \epsilon_{\text{DTM}} < +0.32$   
m w.e. (section 4.1). The value of -0.41 m w.e. occurs in 2004/05 when snow was present at both ALS flight  
campaigns (Table 5) making up for 37% of the initial mass balance value. Applying the workflow for the spatially  
distributed density conversion (section 4.2) leads to  $-0.04 < \epsilon_{\text{r}} < +0.31$  m w.e., with maxima in 2002/03 and 2005/06  
(Table 5). These maxima are due to the total lack of snow and firn at the end of these mass balance years. The uncertainty



345 related to our density assumption (section 4.2) is between  $\pm 0.01 < \sigma_{\kappa} < \pm 0.18$  m w.e. with  $\pm 0.22$  m w.e. over the entire period  
 of record. As dates of the ALS campaigns diverge from the end of the hydrological year a survey date correction is required.  
 Values for related adjustments are in the order of  $-0.08 < \epsilon_{\text{survey}} < +0.06$  m w.e. (section 4.3 and Table 5). Significant melt  
 amounts between ALS flight and field survey dates occur on small parts of the glacier tongue only. E.g. a nearly 1 m ice  
 ablation at the lowest stakes of Hintereisferner measured between 30<sup>th</sup> September (field survey) and 8<sup>th</sup> October (ALS  
 350 campaign) 2006 corresponds to a glacier wide specific mass loss of only 0.03 m w.e. during the same time.

The differences related to the consideration of crevasses ( $\epsilon_{\text{crev}}$ ) in the geodetic method are insignificantly small and vary  
 between  $-0.04$  and  $+0.06$  m w.e. with  $+0.05$  m w.e. for the 2001 to 2011 period (section 4.4 and Table 5). While the glacier  
 wide effect of internal mass changes is small on an annual basis ( $\epsilon_{\text{int}} = +0.05$  m w.e. a<sup>-1</sup>), it is significant on the decadal  
 timescale ( $+0.50$  m w.e.) (section 4.5 and Table 5).

355 Annual totals for method-inherent differences ( $\epsilon_{\text{geod}}$ ) are in the range of  $-0.40$  to  $+0.57$  m w.e. and accumulate to  
 $+0.28$  m w.e. for the 2001 to 2011 period while the respective uncertainties are  $\pm 0.07 < \sigma_{\text{geod}} < \pm 0.20$  m w.e. and  
 $\pm 0.51$  m w.e. for the cumulated values. The 2001 to 2011 one step application of the geodetic method shows  
 $\epsilon_{\text{geod}} = +0.77$  m w.e. and  $\sigma_{\text{geod}} = \pm 0.20$  m w.e. All applied corrections accounting for method inherent differences ( $\epsilon$ ) as well  
 as numbers for related uncertainties ( $\sigma$ ) are summarized in Table 5. Figure 4 shows the vertical profiles of the now corrected  
 360 glaciological and geodetic mass balances for each year from 2001/02 to 2010/11.

The geodetic mass balance of Hintereisferner corrected for  $\epsilon_{\text{geod}}$  for the ten years' period 2001 to 2011 is  $-12.99$   
 $\pm 0.51$  m w.e. and  $-12.45 \pm 0.20$  m w.e. for the 2001 to 2011 one step analysis (Table 6). In turn, the homogenized  
 glaciological mass balance series ( $-12.04 \pm 0.65$  m w.e.) is  $0.95$  m w.e. and  $0.31$  m w.e. less negative respectively. Figure 5  
 depicts the annual glaciological versus geodetic mass balances and their uncertainty ranges. All but three annual data pairs  
 365 match satisfyingly within the assessed uncertainty ranges. The largest positive differences ( $b_{\text{glac}} - b_{\text{geod}} = \Delta b$ ) between the  
 two methods occur in the balance years 2002/03 with  $\Delta b = +0.92$  m w.e. and 2005/06 with  $\Delta b = +0.60$  m w.e. respectively.  
 In 2006/07 the difference between glaciological and geodetic method is  $-0.45$  m w.e., which means the geodetic result is less  
 negative than the glaciological one. Note that the three years displaying the largest differences are at the same time the years  
 with the most negative annual balances.

370 Following Zemp et al. (2013) we perform a statistical significance test with

$$\delta = \frac{\Delta b}{\sqrt{\sigma_{\text{glac}}^2 + \sigma_{\text{geod}}^2}}, \quad (7)$$

where the term  $\sqrt{\sigma_{\text{glac}}^2 + \sigma_{\text{geod}}^2}$  represents the common variance ( $\sigma_{\text{comvar}}$ ) defined as the RSS of the method-inherent  
 uncertainties (Table 6). The more consistent the two methods, the closer  $\delta$  is to zero and the null-hypothesis ( $H_0$ ) on the 95%  
 confidence level to be accepted.



375 As  $\delta$  falls within the 95% confidence interval ( $|\delta| < 1.96$ ) for seven annual and the cumulative mass balance values, the two  
applied methods can be considered as statistically coherent. Hence, for these years, the glaciological method accurately  
captures the annual mass changes at Hintereisferner. From the common variance it is also possible to calculate the smallest  
bias that could theoretically be detected in the glaciological record. The bias calculated at the 5% risk limit lies between 0.79  
and 1.03 m w.e. a<sup>-1</sup> and far above the uncertainty of 0.21 m w.e. a<sup>-1</sup> in the glaciological balance measurements. In contrast,  
380 the detectable bias decreases with the length of the analysed period, which can be explained by error propagation. However,  
it is not possible to statistically identify any biases that might explain the observed discrepancies in the mass balance years  
2002/03, 2005/06 and 2006/07 (see Figure 5).

In search for possible causes of these discrepancies we explore the parameter space in which individual components of  $\epsilon_{\text{geod}}$   
vary. The influence of temporary snow cover ( $\epsilon_{\text{DTM}}$ ) on the geodetic mass balances is high and a thorough consideration  
385 ensures that the results are within the 95% confidence interval. In contrast, the survey date differences show little effect.

Concerning the conversion of glacier volume to mass changes, we used a new classification approach and a dimensionless  
conversion factor ( $\kappa$ ). Calculated values for  $\kappa$  correspond to densities in the range of 820–930 kg m<sup>-3</sup>. This is in line with a  
generally recommended glacier-wide value of 850±60 kg m<sup>-3</sup> (Huss, 2013). Nevertheless, in 2010  $\kappa$  reaches 930, a value  
which at a first glance appears unrealistic. In this year opposite signs of elevation changes in the accumulation and ablation  
390 area compensate for each other, which results in a conversion factor which is higher than the density of ice. Such is possible  
in cases of (i) short observation periods (1–3 years), (ii) small volume changes, (iii) strong year to year changes in the  
vertical mass balance gradients, or combinations of these factors. Our approach accounts for year to year changes in the  
spatial extent and distribution of the snow/firn zones. Highest uncertainties arise in years 2002/03 and 2005/06 when all  
snow from the previous winter melted entirely. As the uncertainty associated with density is of particular importance  
395 (Moholdt et al., 2010; Huss, 2013) we conducted a sensitivity test for the periods of good agreement by holding all other  
parameters fixed. Densities calculated within our  $\kappa$ -range (Table 5) still lead to results within the 95% confidence interval.

As crevasses may influence geodetically calculated volume changes we assessed their impact on the geodetic method. The  
largest impact (0.06 m w.e., or 3% of glaciological mass balance) was detected for 2002/03 when numerous crevasses  
opened due to the extremely hot summer causing extraordinary high glacier velocities (Geist and Stötter, 2007). Hence,  
400 crevasses contribute negligibly to the differences between geodetic and glaciological mass balances.

Internal and basal fluxes are also of rather minor importance (–0.05 m w.e. a<sup>-1</sup>; section 4.5) and do not change the differences  
between the two data series substantially. Yet, we note that in years with extreme melt rates as in 2003 and 2006 meltwater  
penetrates the glacier body during the ablation season and leads to the internal melt rates possibly exceeding the above  
estimate. However even a doubling to –0.10 m w.e. a<sup>-1</sup> does not explain the large discrepancies between the glaciological  
405 and geodetic method in the years 2002/03, 2005/06 and 2006/07.



Other uncertainties possibly contributing to the high mass balance discrepancies in 2002/03, 2005/06 and 2006/07 may be method-inherent uncertainties related to the field measurements, such as the false determination of the last year's summer surface. This might be an issue for the high discrepancies in the individual survey years, but cannot be quantified due to the lack of corresponding information.

410 However, none of the discussed method-inherent uncertainties can explain the considerable high differences in the mass balance years 2002/03, 2005/06 and 2006/07. Nevertheless, a first hint for a potential reason is given by looking at the spatial mass balance distribution as shown in Figure 6 for the exemplary 2002/03.

In all three years glaciological point data from elevations above 3000 m a.s.l. are basically missing on Hintereisferner, but all three years of concern are among the most negative ones (Figure 7). After several years of gradual degradation of the firn  
415 body, ice had suddenly become exposed over all altitude bands by mid of August 2003 with consequent effects on albedo and the energy budget. From then on, the East and South facing high slopes of Hintereisferner had been exposed with a very low albedo to high solar radiation for 6 to 7 weeks of the exceptionally warm and dry summer 2003 (Fink et al., 2004). As a consequence, the mass loss in the former accumulation area of Hintereisferner became large and almost constant above 2800 m a.s.l. (> 50% of the glacier area). This effect had been observed on a smaller glacier some years earlier (Kaser et al.,  
420 2001). By facing this sudden change of the mass balance regime in 2002/03 and the mass balance network not being adapted in time, ablation rates measured at the highest stakes on the flat tongue (at about 3000 m a.s.l.) had been multiplied with the observed ice exposure time of the higher slopes (G. Markl, personal communication). The thereby disregard of higher solar radiation intensity on the slopes compared to the flat tongue are considered to be a possible reason for the differences between the two methods.

425 While higher winter snow cover buried the dark ice surface far enough into the autumns of 2004 and 2005 the high glacier portions remained protected, even allowing obtaining snow pits at the end of summer.

In the hot July of 2006 dark ice became again exposed and the 2002/03 problem was repeated. In 2006/07 when the glaciological mass balance obtains more negative values than the geodetic one we face a different situation. In summer 2007 there was a number of snow falls leading to high surface albedo in the upper part of Hintereisferner while stake  
430 measurements in the lower part of the glacier indicated relatively high ablation rates. The lack of metadata for this particular year disables any further discussion and interpretation. In 2002/03, 2005/06 and 2006/07 we argue for the geodetic data being closer to reality than the glaciological ones as recommended by Thibert et al. (2008) and Huss et al. (2009). For all other years where differences between the methods are statistically insignificant and where error bars overlap we keep the glaciological data in the record. The crucial effect of replacing the three problematic years is well emphasized in the  
435 cumulative mass balance curves shown in Figure 8.

Additional confidence for our approach comes from comparing the 2002/03, 2005/06 and 2006/07 mass balances of Hintereisferner with that of Silvrettagletscher (2.7 km<sup>2</sup>, Switzerland, 52 km away), Jamtalferner (3.7 km<sup>2</sup>, Austria, 45 km),



Weißbrunnferner (0.5 km<sup>2</sup>, Italy, 35 km) and Vernagtferner (7.9 km<sup>2</sup>, Austria, 6 km). While in the years 2002/03 and 2006/07 original Hintereisferner values lay outside the spread of the other glaciers' mass balances and the reanalysed ones are inside, the 2005/06 originals are inside and the reanalysed value becomes the most negative one in Figure 9. This is of no surprise with Hintereisferner being the lowest reaching glacier of all and among the most negative result in all analysed years. A more comprehensive discussion and justification for the different relative positions in Figure 9 would require a detailed investigation on local conditions including meteorological patterns for each individual glacier and mass balance year.

## 445 **6 Conclusions**

Over the past decades it has become a standard procedure to review the annual glaciological data alongside with decadal geodetic mass balances from a variety of sources (e.g., Kuhn et al. 1999; Hagg et al., 2004; Cox and March, 2004; Thibert et al., 2008; Huss et al., 2009; Fischer, 2011; Galos et al. 2017). None of the mentioned studies uses annually obtained geodetic data series. Geist and Stötter (2007) were the first and so far only authors comparing glaciological and geodetic results on an annual timescale for 2001 to 2005. Their findings reveal considerable differences, especially in the year 2002/03. Yet, the study focuses on methodical issues only and does not aim at re-analysing the glaciologically obtained mass balances. It does neither include a thorough data homogenisation nor a robust uncertainty discussion.

In our review of the 2001 to 2011 Hintereisferner mass-balance record we showed that the consideration of method-inherent differences, such as snow cover, survey dates and density assumptions, is mandatory for accurately calculating annual geodetic mass balances. In turn, crevasses and internal processes seem not to play a key role. The largest potential source for differences between the geodetic and glaciological method on the annual scale is the presence of a snow cover. Our method allows us to correct for method-inherent differences for every pixel and provides an appropriate basis for detecting discrepancies in the direct glaciological method. However, our reanalysis approach requires a variety of meta-information and raw data, which can limit its applicability to other sites or cases. However, the corrected geodetic data series show that the glaciological method successfully captures the mass change in seven out of ten mass balance years and both methods generally agree on the annual as well as decadal time scale.

Our analysis shows that in years with very negative mass balances and a low extent of the accumulation area, the glaciological measurement network has to be adapted accordingly. In the case of Hintereisferner, this means that additional ablation stakes in higher parts of the glacier are needed to properly assess the mass changes in regions where snow measurements could be performed in former times. Missing these changes, a resulting lack of respective data is often tried to overcome with different mass balance extrapolation approaches. In the 2001 to 2011 Hintereisferner series the application of such approaches led to considerable deviations from the geodetic results in three years and the careful revision of both series gives support for favouring the geodetic data. Hence, we conclude that in times of increasing availability of high resolution



topographic data, geodetic mass balances can represent a valuable possibility to overcome shortcomings in the glaciological  
470 measurements even on an annual scale if these data are thoroughly analysed.

Although major discrepancies between the glaciological and geodetic methods on Hintereisferner could be explained by our  
workflow, further glaciological investigations should address a better quantification of error sources, such as internal and  
basal processes, in both the glaciological as well as geodetic mass balances. Moreover, in times of vanishing firn areas and  
disconnecting glacier tributaries, existing measurement networks might have to be reassessed.

475 With the high-quality DTMs (e.g. ALS derived DTMs) reliably reproducing the annual mass balance the here presented  
workflow is recommended for i) a re-analysis of annual glaciological with annual geodetic data and ii) as a grid based tool  
for a glacier-wide geodetic mass balance of high spatial resolution suitable for a better understanding of the nature of the  
differences in the two methods.

480

**Acknowledgments:** The ALS data are hosted at the Institute of Geography of the University of Innsbruck and were acquired  
during different scientific projects: The EU-project OMEGA – Operational Monitoring of European Glacial Areas (project-  
no.: EVK2-CT-200-00069), the asap – Austrian Space Applications Programme ALS-X (project-no.: 815527), the ACRP –  
Austrian Climate Research Programmes C4AUSTRIA (project-no.: A963633).

485 Mass balance data, field survey minutes and meteorological data are provided from the Institute of Atmospheric and  
Cryospheric Sciences of the University of Innsbruck. Glaciological mass balance acquisition is funded by the Tyrolean  
Hydrological Survey (Hydrographischer Dienst Tirol).



## References

- 490 Abermann, J., Lambrecht, A., Fischer, A., and Kuhn, M.: Quantifying changes and trends in glacier area and volume in the Austrian Ötztal Alps (1969-1997-2006), *The Cryosphere*, 3, 205–215, doi: 10.5194/tc-3-205-2009, 2009.
- Abermann, J., Fischer, A., Lambrecht, A., and Geist, T.: On the potential of very high-resolution repeat DEMs in glacial and periglacial environments, *The Cryosphere*, 4, 53-65, doi: 10.5194/tc-4-53-2010, 2010.
- Albrecht, O., Jansson, P., and Blatter, H.: Modelling glacier response to measured mass balance forcing, *Ann. Glaciol.*, 31, 495 91–96, doi: 10.3189/172756400781819996, 2000.
- Ambach, W. and Eisner, H.: Analysis of a 20 m. firn pit on the Kesselwandferner (Ötztal Alps). 6, *Journal of Glaciology*, 6(44), 223-231, 1966.
- Andreassen, L. M.: Comparing traditional mass balance measurements with long-term volume change extracted from topographic maps: a case study of Storbreen glacier in Jotunheimen, Norway, for the period 1940–1997, *Geogr. Ann.*, 500 81A(4), 467–476, 1999.
- Andreassen, L. M., Elvehøy, H., Kjølmoen, B., and Engeset, R. V.: Reanalysis of long-term series of glaciological and geodetic mass balance for 10 Norwegian glaciers, *The Cryosphere*, 10, 535-552, doi:10.5194/tc-10-535-2016, 2016.
- Anonymous: Mass-balance terms. *J. Glaciol.*, 8(52), 3–7, 1969.
- Bliss, A., Hock, R., and Radić, V.: Global response of glacier runoff to twenty-first century climate change. *J. Geophys. Res.: Earth Surf.*, 119 (4), 717–730, doi: 10.1002/2013JF002931, 2014.
- Bollmann, E., Sailer, R., Briese, C., Stötter, J., and Fritzmann, P.: Potential of airborne laser scanning for geomorphologic feature and process detection and quantifications in high alpine mountains. *Zeitschrift für Geomorphologie*, 55/2, 83–104, doi:10.1127/0372-8854/2011/0055S2-0047, 2011.
- Bojinski, S., Verstraete, M., Peterson, T.C., Richter, C., Simmons, A., and Zemp, M.: The concept of Essential Climate Variables in Support of climate research, applications, and policy. *Bull. Am. Meteorol. Soc.*, 95 (9), 1431–1443, doi: 10.1175/BAMS-D-13-00047.1, 2014.
- Cogley, J.: Geodetic and direct mass-balance measurements: comparison and joint analysis, *Annals of Glaciology*, 50, 96–100, doi:10.3189/172756409787769744, 2009.
- Cogley, J. G., Hock, R., Rasmussen, L. A., Arendt, A. A., Bauder, A., Braithwaite, R. J., Jansson, P., Kaser, G., Möller, M., 515 Nicholson, L., and Zemp, M.: Glossary of Glacier Mass Balance and Related Terms, IHP-VII Technical Documents in Hydrology No. 86, IACS Contribution No. 2, Paris, UNESCO-IHP, 114 pp., 2011.



- Cox, L. H. and March, R. S.: Comparison of geodetic and glaciological mass-balance techniques, Gulkana Glacier, Alaska, USA, *Journal of Glaciology*, 50(8), 363–370, doi:10.3189/172756504781829855, 2004.
- Cuffey, K. and Paterson, W. S. B.: *The physics of glaciers*, 5th Edn., Massachusetts Academic Press, Burlington, 704 pp., 520 2010.
- Fink, A., Brücher, T., Krüger, A., Leckebusch, G., Pinto, J., and Ulbrich, U.: The 2003 European summer heatwaves and drought—synoptic diagnosis and impacts. *Weather* 59: 209–216, doi:10.1256/wea.73.04, 2004.
- Fischer, A.: Comparison of direct and geodetic mass balances on a multi-annual time scale, *The Cryosphere*, 5, 107–124, doi:10.5194/tc-5-107-2011, 2011.
- 525 Fischer, A., Seiser, B., Stocker Waldhuber, M., Mitterer, C., and Abermann, J.: Tracing glacier changes in Austria from the Little Ice Age to the present using a lidar-based high-resolution glacier inventory in Austria, *The Cryosphere*, 9, 753–766, doi:10.5194/tc-9-753-2015, 2015.
- Fountain, A. G., Jansson, P., Kaser, G., and Dyurgerov, M.: Summary of the workshop on methods of mass balance measurements and modelling, Tarfala, Sweden, August 10–12, 1998, *Geogr. Ann.*, 81A(4), 461–465, doi:10.1111/1468-530 0459.00075, 1999.
- Fountain, A. G. and Vecchia, A.: How many stakes are required to measure the mass balance of a glacier? *Geogr. Ann.*, 81A(4), 563–573, doi:10.1111/1468-0459.00084, 1999.
- Frei, C. and Schär, C.: A precipitation climatology of the Alps from high-resolution rain-gauge observations. *Int. J. Climatol.*, 18, 873–900, doi: 10.1002/(SICI)1097-0088(19980630)18, 1998.
- 535 Fritzmann, P., Höfle, B., Vetter, M., Sailer, R., Stötter, J., and Bollmann, E.: Surface classification based on multi-temporal airborne LiDAR intensity data in high mountain environments – A case study from Hintereisferner, Austria. *Zeitschrift für Geomorphologie*, 55/2, 105–126, doi: 10.1127/0372-8854/2011/0055S2-0048, 2011.
- Gardner, A. S., Moholdt, G., Cogley, J. G., Wouters, B., Arendt, A. A., Wahr, J., Berthier, E., Hock, R., Pfeffer, W. T., Kaser, G., Ligtenberg, S. R. M., Bolch, T., Sharp, M. J., Hagen, J. O., van den Broeke, M. R. and Paul, F.: A reconciled estimate of glacier contributions to sea level rise: 2003 to 2009, *Science*, 340, 852–857, doi:10.1126/science.1234532, 2013.
- 540 Galos, S. P., Klug, C., Maussion, F., Covi, F., Nicholson, L., Rieg, L., Gurgiser, W., Mölg, T., and Kaser, G.: Reanalysis of a ten year record (2004–2013) of seasonal mass balances at Langenferner/Vedretta Lunga, Ortler-Alps, Italy, *The Cryosphere*, 11, 1417–1439, <https://doi.org/10.5194/tc-11-1417-2017>, 2017.
- Geist, T. and Stötter, J.: Documentation of glacier surface elevation change with multitemporal airborne laser scanner data – case study: Hintereisferner and Kesselwandferner, Tyrol, Austria, *Zeitschrift für Gletscherkunde und Glazialgeologie*, 41, 77–106, 2007.



- Geist, T. and Stötter, J.: Airborne laser scanning in glacier studies. In: Pellika, P. and Rees, W. G. (eds.), *Remote Sensing of Glaciers. Techniques for Topographic, Spatial and Thematic Mapping of Glaciers*. London, pp. 179–194, 2010.
- Haeberli, W.: Historical evolution and operational aspects of worldwide glacier monitoring, in: *Into the second century of worldwide glacier monitoring: Prospects and strategies*, edited by: Haeberli, W., Hoelzle, M. and Suter, S., UNESCO-IHP, Paris, France, 35–51, 1998.
- Hagg, W., Braun, L., Uvarov, V., and Makarevich, K.: A comparison of three methods of mass balance determination in the Tuyuksu glacier region, Tien Shan, Central Asia, *J. Glaciology*, 50, 171, 505–510, doi:10.3189/172756504781829783, 2004.
- Haug, T., Rolstad, C., Elvehøy, H., Jackson, M., and Maalen-Johansen, I.: Geodetic mass balance of the western Svartisen ice cap, Norway, in the periods 1968–1985 and 1985–2002, *Ann. Glaciol.*, 50, 119–125, 2009.
- Herron, M. M. and Langway, C. C.: Firn densification: an empirical model. *J. Glaciol.* 25, 373–385, 1980.
- Höfle, B. and Pfeifer, N.: Correction of laser scanning intensity data: Data and model-driven approaches. *ISPRS Journal of Photogrammetry and Remote Sensing*, 62(6), pp. 415–433, doi:10.1016/j.isprsjprs.2007.05.008, 2007.
- Hoinkes, H.: Methoden und Möglichkeiten von Massenhaushaltsstudien auf Gletschern, *Zeitschrift für Gletscherkunde und Glazialgeologie*, 6, 37–90, 1970.
- Holmlund, P.: Mass balance of Storglaciären during the 20th century, *Geogr. Ann.*, 69A(3–4), 439–447, doi:10.2307/521357, 1987.
- Huss, M., Bauder, A., and Funk, M.: Homogenization of longterm mass-balance time series, *Ann. Glaciol.*, 50(9), 198–206, doi:10.3189/172756409787769627, 2009.
- 565 Huss, M. and Hock, R.: A new model for global glacier change and sea-level rise. *Frontiers in Earth Science*, 3:54, doi:10.3389/feart.2015.00054, 2015.
- Huss, M.: Present and future contribution of glacier storage change to runoff from macroscale drainage basins in Europe. *Water Resour. Res.*, 47 (7), W07511. doi: 10.1029/2010WR010299, 2011.
- Huss, M.: Density assumptions for converting geodetic glacier volume change to mass change, *The Cryosphere*, 7, 877–887, doi:10.5194/tc-7-877-2013, 2013.
- 570
- Jansson, P.: Effect of uncertainties in measured variables on the calculated mass balance of Storglaciären, *Geogr. Ann.*, 81A, 633–642, doi:10.1111/1468-0459.00091, 1999.
- Joerg, P. C., Morsdorf, F., and Zemp, M.: Uncertainty assessment of multi-temporal airborne laser scanning data: A case study on an Alpine glacier, *Remote Sens. Environ.*, 127, 118–129, 2012.



- 575 Kaser, G., Zingerle C., Oberschmied C., and Munari M.: An exceptionally negative mass-balance of a small Alpine glacier. *Geografia Fisica e Dinamica Quaternaria* V: 99-102, 2001.
- Kaser, G., Fountain, A. G., and Jansson, P.: A manual for monitoring the mass balance of mountain glaciers with particular attention to low latitude characteristics. A contribution to the UNESCO HKH-Friend programme, Paris, France, 107 pp., 2003.
- 580 Kaser, G., Cogley, J., Dyurgerov, M., Meier, M., and Ohmura, A.: Mass balance of glaciers and ice caps: Consensus estimates for 1961–2004, *Geophys. Res. Lett.*, 33, 19501, doi:10.1029/2006GL027511, 2006.
- Kaser, G., Großhauser, M., and Marzeion, B.: Contribution potential of glaciers to water availability in different climate regimes. *Proceedings of the National Academy of Sciences*, 20223 – 20227, doi: 10.1073/pnas.1008162107, 2010.
- Koblet, T., Gärtner-Roer, I., Zemp, M., Jansson, P., Thee, P., Haeberli, W., and Holmlund, P.: Reanalysis of multi-temporal aerial images of Storglaciren, Sweden (1959–99) – Part 1: Determination of length, area, and volume changes, *The Cryosphere*, 4, 333–343, doi:10.5194/tc-4-333-2010, 2010.
- Kodde, M. P., Pfeifer, N., Gorte, B. G. H., Geist, T., and Höfle, B.: Automatic Glacier Surface Analysis from Airborne Laser Scanning. In: *IAPRS Volume XXXVI, Part 3*: 221–226, 2007.
- Krimmel, R. M.: Analysis of Difference between Direct and Geodetic Mass Balance Measurements at South Cascade Glacier, Washington, *Geogr. Ann. A*, 81(4), 653–658, doi:10.1111/1468-0459.00093, 1999.
- 590 Kuhn, M., Dreiseitl, E., Hofinger, S., Markl, G., Span, N., and Kaser, G.: Measurements and models of the mass balance of Hintereisferner, *Geogr. Ann. A*, 81A, 659–670, doi:10.1111/1468-0459.00094, 1999.
- Lang, H. and Patzelt, G.: Die Volumenänderungen des Hintereisferners (Ötztaler Alpen) im Vergleich zur Massenänderung im Zeitraum 1953–64, *Zeitschrift für Gletscherkunde und Glazialgeologie*, 7(1–2), 229–238, 1971.
- 595 Lliboutry, L.: Multivariate statistical analysis of glacier annual balances. *J. Glaciol.*, 13, 69, 371–392, doi:10.3198/1974JoG13-69-371-392, 1974.
- Marzeion, B., Jarosch, A. H., and Hofer, M.: Past and future sea-level change from the surface mass balance of glaciers, *The Cryosphere*, 6, 1295–1322, doi:10.5194/tc-6-1295-2012, 2012.
- Marzeion, B., Jarosch, A. H., and Gregory, J. M.: Feedbacks and mechanisms affecting the global sensitivity of glaciers to climate change, *The Cryosphere*, 8, 59–71, doi:10.5194/tc-8-59-2014, 2014.
- 600 Mayo, L.R.: Internal ablation – an overlooked component of glacier mass balance. (abstract) *EOS, Transactions, American Geophysical Union*, 73(43) Supplement: 180, 1992.



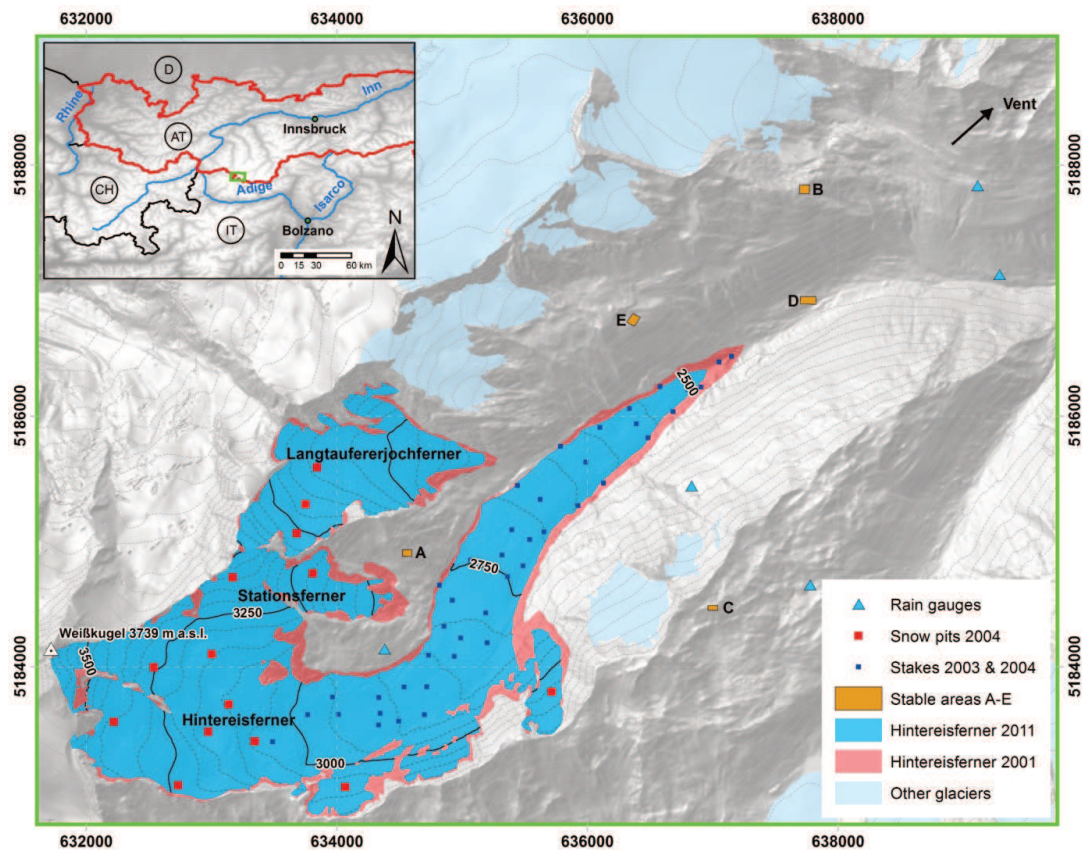
- Medici, F. and Rybach, L.: Geothermal map of Switzerland 1:500'000 (Heat Flow Density). *Beitr. Geol. Schweiz, Ser. Geophys.* Nr. 30, 36 p, 1995.
- 605 Mengel, M., Levermann, A., Frieler, K., Robinson, A., Marzeion, B., and Winkelmann, R.: Future sea level rise constrained by observations and long-term commitment. *Proc Natl Acad Sci.* doi: 10.1073/pnas.1500515113, 2016.
- Moholdt, G., Nuth, C., Hagen, J.O., and Kohler, J.: Recent elevation changes of Svalbard glaciers derived from ICESat laser altimetry. *Remote Sens. Environ.*, 114(11), 2756–2767, 2010.
- Nuth, C. and Kääb, A.: Co-registration and bias corrections of satellite elevation data sets for quantifying glacier thickness change, *The Cryosphere*, 5, 271–290, doi:10.5194/tc-5-271-2011, 2011.
- 610 Oerlemans, J.: A note on the water budget of temperate glaciers, *The Cryosphere*, 7, 1557–1564, doi:10.5194/tc-7-1557-2013, 2013.
- Östling, M. and Hooke, R. LeB.: Water storage in Storglaciären, Kebnekaise, Sweden, *Geogr. Ann.* 68A(4), 279–290, 1986.
- Østrem, G. and Brugman, M.: Glacier mass-balance measurements: A manual for field and office work, NHRI Science Report, Saskatoon, Canada, 224 pp., 1991.
- 615 Østrem, G. and Haakensen, N.: Map comparison of traditional mass-balance measurements: which method is better?, *Geogr. Ann. A*, 81, 703–711, 1999.
- Radic, V. and Hock, R.: Modeling future glacier mass balance and volume changes using ERA-40 reanalysis and climate models: A sensitivity study at Storglaciären, Sweden, *Journal of Geophysical Research*, 111, F03003, doi:10.1029/2005JF000440, 2006.
- 620 Radić, V., Bliss, A., Beedlow, A. C., Hock, R., Miles, E., and Cogley, J. G.: Regional and global projections of 21st century glacier mass changes in response to climate scenarios from global climate models. *Climate Dynamics*. doi:10.1007/s00382-013-1719-7, 2013.
- Richter, E.: *Die Gletscher der Ostalpen*. 3rd ed., *Handbücher zur Deutschen Landes-und Volkskunde*, Engelhornverlag, Stuttgart, 306 pp, 1888.
- 625 Rieg, L., Wichmann, V., Rutzinger, M., Sailer, R., Stötter, J., and Geist, T.: Data infrastructure for multitemporal airborne LiDAR point cloud analysis - examples from physical geography in high mountain environments. *Computers, Environment and Urban Systems*. 45: 137-146, doi:10.1016/j.compenvurbsys.2013.11.004, 2014.
- Paterson, W. S. B.: *The physics of glaciers*, 3rd edition, Pergamon Press, Oxford, 480 pp, 1994.
- 630 Patzelt, G.: Glacier advances in the Alps 1965 to 1980. *Z. f. Gletscherkunde u. Glazialgeologie*, Bd.21, H.1/2 (1985): 403-407, 1985.



- Pfeffer, W.T., Meier, M.F., and Illangasekare, T.H.: Retention of Greenland run off by refreezing: implications for projected future sea level change. *J. Geophys. Res.* 96, 22117, doi:10.1029/91JC02502, 1991.
- Prinz, R., Fischer, A., Nicholson, L., and Kaser, G.: Seventy-six years of mean mass balance rates derived from recent and re-evaluated ice volume measurements on tropical Lewis Glacier, Mount Kenya, *Geophysical Research Letters*, 38(20), L20502, doi:10.1029/2011GL049208, 2011.
- Sailer, R., Bollmann, E., Hoinkes, S., Rieg, L., Sproß, M., and Stötter, J.: Quantification of geomorphodynamic processes in glaciated and recently deglaciated terrain based on airborne laser scanning data. *Geografiska Annaler: Series A, Physical Geography* 94: 17–32. DOI: 10.1111/j.1468-0459.2012.00456.x, 2012.
- 640 Sailer, R., Rutzinger, M., Rieg, L., and Wichmann, V.: Digital elevation models derived from airborne laser scanning point clouds: appropriate spatial resolutions for multi-temporal characterization and quantification of geomorphological processes. *Earth Surface Processes and Landforms* 39 : 272–284. DOI: 10.1002/esp.3490, 2014.
- Sapiano, J., Harrison, W., and Echelmeyer, K.: Elevation, volume and terminus changes of nine glaciers in North America, *J. Glaciol.*, 44, 119–135, 1998.
- 645 Slangen, A.B.A., Adloff, F., Jevrejeva, S., Leclercq, P.W., Marzeion, B., Wada, Y., and Winkelmann, R.: A review of recent updates of sea-level projections at global and regional scales. *Surv. Geophys.*, early on-line, doi:10.1007/s10712-016-9374-2, 2016.
- Sold, L., Huss, M., Machguth, H., Joerg, P. C., Leysinger Vieli, G., Linsbauer, A., Salzmann, N., Zemp, M., and Hoelzle, M.: Mass balance re-analysis of Findelengletscher, Switzerland; benefits of extensive snow accumulation measurements. *Front. Earth Sci.* 4:18. doi:10.3389/feart.2016.00018, 2016.
- 650 Thibert, E., Blanc, R., Vincent, C., and Eckert, N.: Glaciological and volumetric mass balance measurements error analysis over 51 years for the Sarennes glacier, French Alps, *Journal of Glaciology*, 54, 186, 522–532(11), doi:10.3189/002214308785837093, 2008.
- Thibert, E. and Vincent, C.: Best possible estimation of mass balance combining glaciological and geodetic methods, *Ann. Glaciol.* 50, 112–118, doi:10.3189/172756409787769546, 2009.
- Vaughan, D., Comiso, J., Allison, I., Carrasco, J., Kaser, G., Kwok, R., Mote, P., Murray, T., Paul, F., Ren, J., Rignot, E., Solomina, O., Steffen, K., and Zhang, T.: Observations: cryosphere, in: *Climate Change 2013: the Physical Science Basis. Contribution of Working Group I to the Fifth Assessment Report of the Intergovernmental Panel on Climate Change*, edited by: Stocker, T., Qin, D., Plattner, G.-K., Tignor, M., Allen, S., Boschung, J., Nauels, A., Xia, Y., Bex, V., and Midgley, P., Cambridge University Press, Cambridge, UK, New York, NY, USA, 317–382, 2013
- 660



- Weber, M., Braun, L.N., Mauser, W., and Prasch, M.: Contribution of rain, snow- and ice melt in the Upper Danube discharge today and in the future. *Geogr. Fis. Din. Quat.*, 33 (2), 221–230, 2010.
- Wever, C. and Lindenberger, J.: Laser scanning – a mapping method gains ground. *Photogrammetric Week*, 99, 125–132, 1999.
- 665 Zemp, M., Hoelzle, M., and Haeberli, W.: Six decades of glacier mass-balance observations: a review of the worldwide monitoring network, *Ann. Glaciol.*, 50(50), 101–111, 2009.
- Zemp, M., Jansson, P., Holmlund, P., Gärtner-Roer, I., Koblet, T., Thee, P., and Haeberli, W.: Reanalysis of multi-temporal aerial images of Storglaciren, Sweden (1959–99) – Part 2: Comparison of glaciological and volumetric mass balances. *Cryosphere*, 4, 345–357, doi:10.5194/tc-4-345-2010, 2010.
- 670 Zemp, M., Thibert, E., Huss, M., Stumm, D., Rolstad Denby, C., Nuth, C., Nussbaumer, S.U., Moholdt, G., Mercer, A., Mayer, C., Joerg, P.C., Jansson, P., Hynek, B., Fischer, A., Escher-Vetter, H., Elvehøy, H., and Andreassen L.M.: Reanalysing glacier mass balance measurement series, *Cryosphere*, 7, 1227–1245, doi:10.5194/tc-7-1227-2013, 2013.



675 Figure 1: A map of Hintereisferner with the locations of the rain gauges and the glaciological mass balance measurement points in 2004 as an example. Also depicted are the glacier outlines for 2001 and 2011. Note that in 2003 no accumulation measurements have been carried out, thus, only the ablation stakes were available. Coordinates are in WGS84/UTM32N.

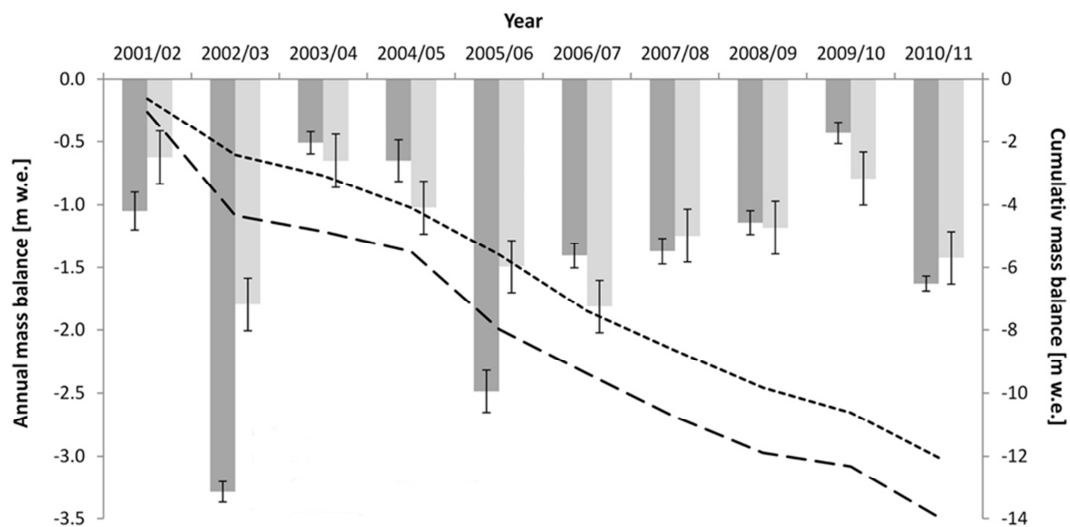


Figure 2: First order comparison of the annual and cumulative area adjusted glaciological (bglac\_hom; light grey bar and dotted black line) and raw geodetic mass balances (bgeod\_raw; dark grey bar and dashed black line) of Hintereisferner in the period from 2001 to 2011.

680 Method-inherent uncertainties ( $\sigma_{DTM}$  for geodetic,  $\sigma_{point}$  and  $\sigma_{spatial}$  for glaciological balances) are indicated by horizontal lines, respectively.

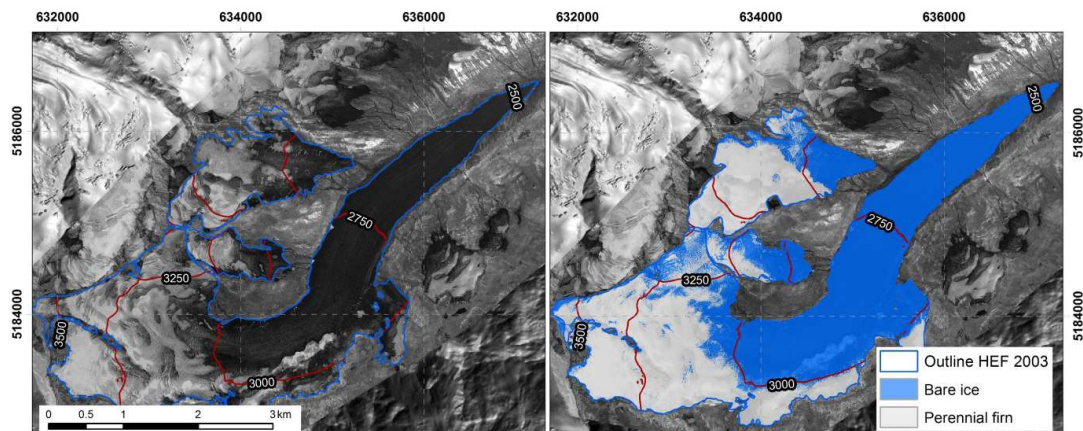
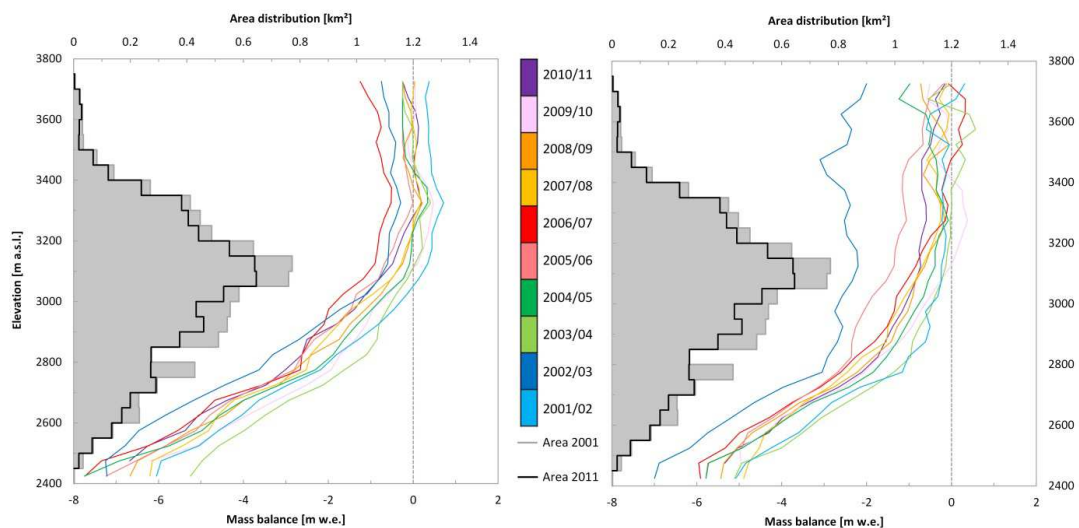
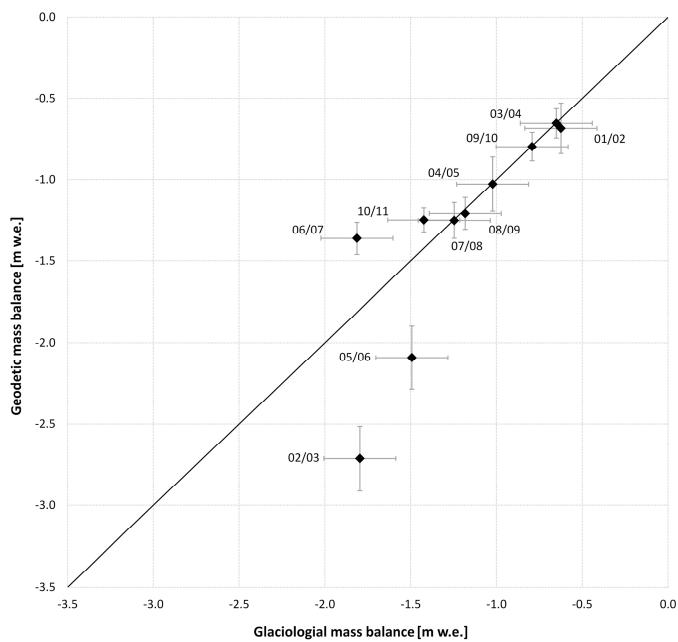


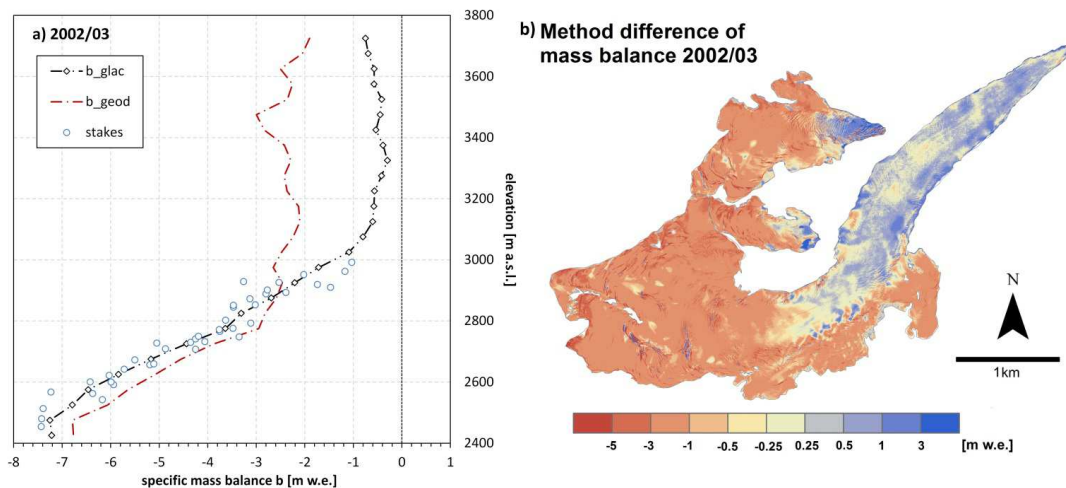
Figure 3: Intensity of the reflected laser beam of the ALS acquisition in 2008 (left) and derived surface classes (right). The classes are perennial firn with an average density of  $700 \pm 50 \text{ kg m}^{-3}$  and bare glacier ice of  $900 \pm 17 \text{ kg m}^{-3}$ . Map coordinates are in WGS84/UTM32N.



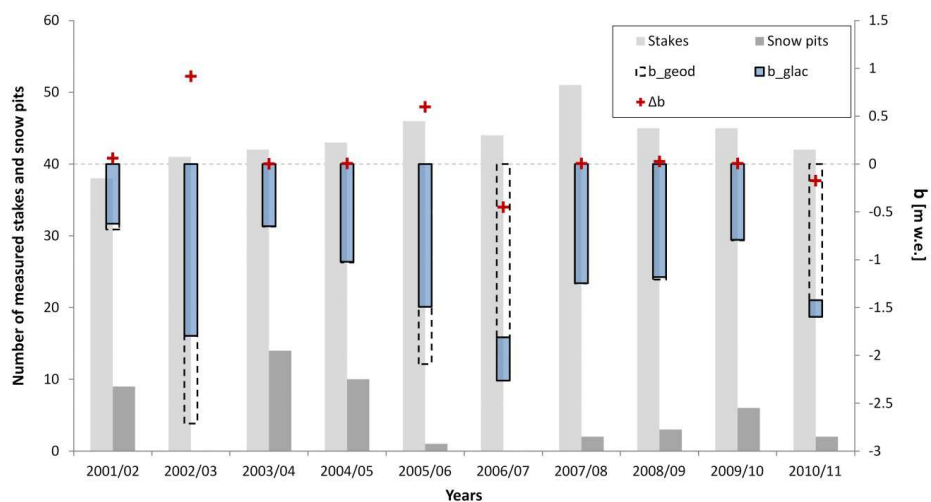
690 Figure 4: Corrected annual glaciological (left) and geodetic (right) vertical mass balance profiles for the period 2001/02–2010/11. Note that highest differences, which occur in the years 2002/03 (dark blue line) and 2005/06 (light red line) are also visible in the balance profiles at elevations above 2900 m a.s.l.



695 Figure 5: Annual glaciological vs. geodetic mass balance. Both series are corrected for method-inherent differences and plotted with uncertainties (grey crosses). The black diagonal line marks equal balances from both methods.



700 Figure 6: The extraordinary mass balance year 2002/03. (a) Comparison of vertical mass ( $b_{glac}$ ;  $b_{geod}$ ) and the distribution of accumulation and ablation measurements. (b) Spatial distributed difference of the methodical results with main deviations between the methods above 3000 m a.s.l. where in situ observations are missing.



705 Figure 7: Comparison of mass balances ( $b_{glac}$ ;  $b_{geod}$ ) and their differences ( $\Delta b$ ) with number of accumulation and ablation measurements.

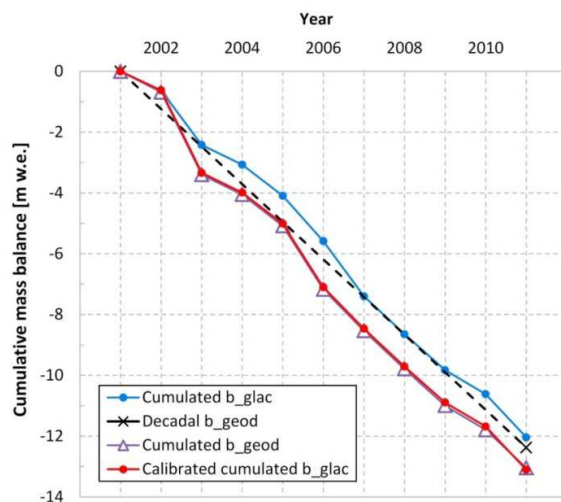


Figure 8: Calibration of glaciological mass balance series for the period 2001–2011 with the geodetic surveys for Hintereisferner. Cumulative adjusted mass balance ( $b_{glac}$ ) is calibrated with the geodetic mass change ( $b_{geod}$ ) for the respective years 2002/03, 2005/06 and 2006/07 resulting in calibrated  $b_{glac}$ .

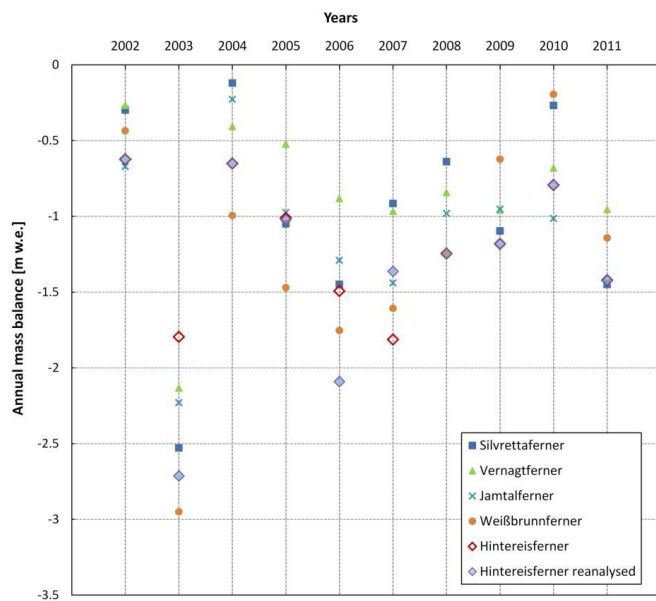


Figure 9: Comparison of original and reanalysed annual glaciological mass balances of Hintereisferner with different glaciers measured in the surrounding of Hintereisferner.



715 Table 1: Key parameters for the 11 ALS data acquisition campaigns at Hintereisferner from 2001 to 2011. Point density is averaged over the study area, while the horizontal accuracy is calculated based on a flat reference area in vicinity of the study area.

Date of acquisition	Optech sensor	Mean height above ground [m]	Max. scanning angle [degrees]	Pulse repetition frequency (Hz)	Across track overlap (%)	Average point density (points/m <sup>2</sup> )	Vertical accuracy standard deviation (SD) (m)
11.10. 2001	ALTM 1225	900	20	25000	24	1.1	n.a.
18.09. 2002	ALTM 3033	900	20	33000	24	1	0.1
26.09. 2003	ALTM 1225	900	20	25000	24	1	0.06
05.10. 2004	ALTM 2050	1000	20	50000	24	2	0.07
12.10. 2005	ALTM 3100	1000	22	70000	50-75	3.4	0.07
08.10. 2006	ALTM 3100	1000	20	70000	37 - 75	2	0.08
11.10. 2007	ALTM 3100	1000	20	70000	37 - 75	3.4	0.06
09.09. 2008	ALTM 3100	1000	20	70000	40 - 45	2.2	0.06
30.09. 2009	ALTM 3100	1100	20	70000	31 - 66	2.7	0.05
08.10. 2010	ALTM Gemini	1000	25	70000	62	3.6	0.03
04.10. 2011	ALTM 3100	1100	20	70000	25 - 75	2.9	0.04



Table 2: Area averaged annual altitudinal changes  $\overline{\Delta z}$  (m) and according standard deviation  $SD\Delta z$  (m) of selected stable areas in the surroundings of Hintereisferner. Bold numbers indicate the existence of snow cover.

$\Delta z$ campaign [m]		01/02	02/03	03/04	04/05	05/06	06/07	07/08	08/09	09/10	10/11	
Stable areas	A	$\overline{\Delta z}$ stable area (A)	<b>-0.38</b>	-0.10	0.00	<b>0.13</b>	<b>-0.58</b>	<b>-0.17</b>	<b>-0.26</b>	0.03	0.15	-0.06
	~3000 m a.s.l.	$SD\Delta z$ surface lowering A	0.03	0.04	0.03	0.06	0.09	0.12	0.06	0.02	0.04	0.03
	B	$\overline{\Delta z}$ stable area (B)	<b>-0.42</b>	-0.14	-0.02	<b>0.17</b>	<b>-0.52</b>	<b>-0.16</b>	<b>-0.18</b>	0.04	0.10	-0.05
	~3100 m a.s.l.	$SD\Delta z$ surface lowering B	0.09	0.03	0.07	0.06	0.12	0.08	0.03	0.03	0.09	0.01
	C	$\overline{\Delta z}$ stable area (C)	<b>-0.46</b>	-0.15	-0.06	-0.06	<b>-0.45</b>	<b>-0.19</b>	-0.07	0.10	0.15	-0.10
	~3200 m a.s.l.	$SD\Delta z$ surface lowering C	0.12	0.02	0.05	0.09	0.07	0.11	0.01	0.04	0.04	0.03
	D	$\overline{\Delta z}$ stable area (D)	-0.14	-0.07	-0.03	0.03	-0.09	-0.01	-0.06	0.05	0.05	-0.11
	~2500 m a.s.l.	$SD\Delta z$ surface lowering D	0.06	0.07	0.02	0.02	0.07	0.05	0.07	0.03	0.03	0.04
	E	$\overline{\Delta z}$ stable area (E)	<b>-0.19</b>	-0.04	-0.04	0.05	<b>-0.39</b>	-0.06	-0.01	-0.02	0.10	-0.13
	~2850 m a.s.l.	$SD\Delta z$ surface lowering E	0.03	0.02	0.03	0.06	0.07	0.05	0.06	0.05	0.03	0.03



Table 3: Original (WGMS) and area adjusted ( $\epsilon_{\text{area}}$ ) and uncertainty assessed ( $\sigma_{\text{glac}}$ ) annual glaciological mass balances ( $b_{\text{glac.hom}}$ ) in comparison to the - DTM uncertainty ( $\sigma_{\text{DTM}}$ ) assessed - raw annual geodetic mass balances ( $b_{\text{geod.raw}}$ ); converted into meter water equivalent (m w.e.) using  $900 \text{ kg m}^{-3}$ , for Hintereisferner from 2001 to 2011.

Period	$b_{\text{glac.WGMS}}$	$\epsilon_{\text{area}}$	$b_{\text{glac.hom}} \pm \sigma_{\text{glac}}$	$b_{\text{geod.raw}} \pm \sigma_{\text{DTM}}$	$b_{\text{glac.hom}} - b_{\text{geod.raw}}$
<b>2001/02</b>	-0.647	+0.023	-0.624 $\pm$ 0.21	-1.049 $\pm$ 0.15	0.425
<b>2002/03</b>	-1.814	+0.018	-1.796 $\pm$ 0.21	-3.285 $\pm$ 0.08	1.489
<b>2003/04</b>	-0.667	+0.016	-0.685 $\pm$ 0.21	-0.509 $\pm$ 0.09	-0.176
<b>2004/05</b>	-1.061	+0.039	-1.033 $\pm$ 0.21	-0.650 $\pm$ 0.16	-0.383
<b>2005/06</b>	-1.516	+0.023	-1.493 $\pm$ 0.21	-2.487 $\pm$ 0.17	0.994
<b>2006/07</b>	-1.798	-0.015	-1.813 $\pm$ 0.21	-1.404 $\pm$ 0.10	-0.409
<b>2007/08</b>	-1.235	-0.011	-1.246 $\pm$ 0.21	-1.369 $\pm$ 0.10	0.123
<b>2008/09</b>	-1.182	0.000	-1.182 $\pm$ 0.21	-1.141 $\pm$ 0.09	-0.041
<b>2009/10</b>	-0.819	+0.027	-0.792 $\pm$ 0.21	-0.430 $\pm$ 0.09	-0.362
<b>2010/11</b>	-1.420	-0.003	-1.423 $\pm$ 0.21	-1.629 $\pm$ 0.06	0.206
<b>01/11</b>	-12.159	+0.117	-12.042 $\pm$ 0.65	-13.343 $\pm$ 0.14	1.301
<b>01-11<sub>cum</sub></b>	-12.159	+0.117	-12.042 $\pm$ 0.65	-13.953 $\pm$ 0.36	1.911



725 Table 4: Summary of ALS and closest field survey dates of Hintereisferner, mean snow cover in DTM ((SC)<sub>ALS</sub>) and in field survey ((SC)<sub>field</sub>) used for DTM correction, values of survey date adjustments ( $\epsilon_{\text{survey}}$ ), glacier area (A) and classified firm area (A<sub>F</sub>). Short comments are taken from field measurement minutes. The mean accumulation area decreased from 3.85 km<sup>2</sup> to 1.98 km<sup>2</sup> for the period 2001–2011.

ALS survey	field survey	$\overline{SC}_{\text{ALS}}$ [m]	$\overline{SC}_{\text{field}}$ [m]	$\epsilon_{\text{survey}}$ [m w.e.]	A [km <sup>2</sup> ]	A <sub>F</sub> [km <sup>2</sup> ]	Comments
11 Oct 2001	8 Oct 2001	0.52	0.47	-0.12	8.02	3.85	Continuous snow cover at field survey (10 – 50 cm, probings < 3400 m a.s.l.); further snowfall between 8 <sup>th</sup> and 11 <sup>th</sup> of October; snow cover estimation based on ALS data
18 Sept 2002	2 Oct 2002	0.00	0.17	+0.08	7.86	3.53	Continuous snow cover at field survey (10 – 35 cm, < 3400 m a.s.l.), snow cover estimation based on field survey and meteorological data
26 Sept 2003	30 Sept 2003	0.00	0.00	-0.02	7.66	3.12	Strong ablation on stakes between 16 <sup>th</sup> August and 30 <sup>th</sup> September; 1 – 4 cm/d below 3000 m a.s.l. estimated based on field survey and meteorological data ; no snow cover at geodetic survey
5 Oct 2004	30 Sept 2004	0.23	0.23	+0.05	7.61	3.05	Continuous snow cover at field survey (5 – 40 cm, < 3400 m a.s.l.); snow cover estimation based on field survey data
12 Oct 2005	30 Sept 2005	0.46	0.30	-0.07	7.51	2.72	Continuous snow cover at field survey (1 – 30 cm, < 3400 m a.s.l.); additional snowfall event between 1 <sup>st</sup> and 12 <sup>th</sup> of October (103 mm on HEF) snow cover estimation based on ALS data
8 Oct 2006	30 Sept 2006	0.13	0.00	-0.01	7.38	2.43	No snow cover at field survey; snowfall events between 3 <sup>rd</sup> and 8 <sup>th</sup> of October (82 mm on HEF); snow cover estimation based on ALS data
11 Oct 2007	1 Oct 2007	0.12	---	-0.01	7.28	2.32	No field survey data available; snowfall events between 1 <sup>st</sup> and 12 <sup>th</sup> of October; snow cover estimation based on ALS data
9 Sept 2008	30 Sept 2008	0.00	0.18	-0.05	7.15	2.03	Continuous snow cover at field survey (0 – 32 cm, < 3400 m a.s.l.); 4 – 28 cm ablation at stakes between 9 <sup>th</sup> and 30 <sup>th</sup> of September; snow cover estimation based on field survey and meteorological data
30 Sept 2009	27 Sept 2009	0.00	0.00	0.00	7.05	2.01	No correction necessary; no significant snow cover < 3400 m a.s.l.
8 Oct 2010	27 Sept 2010	0.26	0.26	-0.03	6.88	2.22	Continuous snow cover at field survey (1 – 42 cm, < 3400 m a.s.l.); snowfall event between 28 <sup>th</sup> of Sept and 8 <sup>th</sup> of October (12 mm on HEF) but nearly no ablation; snow cover estimation based on field data
4 Oct 2011	4 Oct 2011	0.00	0.00	0.00	6.79	1.98	No correction necessary; no significant snow cover < 3400 m a.s.l.



730 Table 5: Quantified method-inherent differences and uncertainties related to DTM ( $\epsilon_{DTM}$  and  $\sigma_{DTM}$ ), density conversion ( $\epsilon_{\kappa}$  and  $\sigma_{\kappa}$ ), survey dates ( $\epsilon_{survey}$ ), internal processes ( $\epsilon_{int}$  and  $\sigma_{int}$ ) and crevasse volume ( $\epsilon_{crev}$ ). While the overall  $\epsilon_{geod}$  accumulates from all individual differences, the overall  $\sigma_{geod}$  is calculated by propagating the individual uncertainties. All units are in meter water equivalent (m w.e.), except of the dimensionless  $\kappa$ .

year	$\kappa$	$\epsilon_{DTM}$	$\epsilon_{\kappa}$	$\epsilon_{survey}$	$\epsilon_{int}$	$\epsilon_{crev}$	$\epsilon_{geod}$	$\sigma_{DTM}$	$\sigma_{\kappa}$	$\sigma_{int}$	$\sigma_{geod}$
<b>01/02</b>	830±30	+0.29	+0.08	-0.03	+0.05	-0.02	+0.36	±0.15	±0.04	±0.015	±0.16
<b>02/03</b>	820±45	+0.09	+0.31	+0.06	+0.05	+0.06	+0.57	±0.08	±0.18	±0.015	±0.20
<b>03/04</b>	875±20	-0.20	+0.01	+0.03	+0.05	-0.04	-0.15	±0.09	±0.01	±0.015	±0.09
<b>04/05</b>	855±30	-0.41	+0.03	-0.02	+0.05	-0.04	-0.38	±0.16	±0.02	±0.015	±0.17
<b>05/06</b>	850±35	+0.29	+0.14	-0.08	+0.05	-0.005	+0.40	±0.17	±0.10	±0.015	±0.19
<b>06/07</b>	885±20	-0.02	+0.02	-0.02	+0.05	+0.004	+0.04	±0.10	±0.01	±0.015	±0.10
<b>07/08</b>	865±25	+0.10	+0.05	-0.06	+0.05	-0.02	+0.12	±0.10	±0.04	±0.015	±0.11
<b>08/09</b>	890±20	-0.05	+0.01	-0.05	+0.05	-0.03	-0.07	±0.09	±0.02	±0.015	±0.10
<b>09/10</b>	930±20	-0.32	-0.03	-0.03	+0.05	-0.04	-0.37	±0.09	±0.02	±0.015	±0.09
<b>10/11</b>	870±25	+0.32	+0.05	+0.03	+0.05	-0.02	+0.43	±0.06	±0.04	±0.015	±0.07
<b>01/11</b>	890±20	+0.29	+0.13	-0.07	+0.50	+0.05	+0.77	±0.14	±0.27	±0.047	±0.20
<b>cum</b>	---	+0.11	+0.69	-0.18	+0.50	-0.15	+0.28	±0.36	±0.22	±0.047	±0.78



735 Table 6: Summary of the statistical comparison of glaciological and geodetic balances of Hintereisferner. The table shows different periods of record with the improved balances ( $b_{\text{geod}}$ ,  $b_{\text{glac}}$ ) and related method-inherent uncertainties ( $\pm\sigma$ ), together with differences ( $\Delta b = b_{\text{glac}} - b_{\text{geod}}$ ), common variance ( $\sigma_{\text{comvar}}$ ), and the statistical significance  $\delta$ . The acceptance of the null-hypothesis ( $H_0$ ), whether the glaciological balance is statistically different from the geodetic balance or not, is evaluated on the 95% confidence level, which corresponds to  $\delta$ -values inside (outside) the  $\pm 1.96$  range, respectively.  $\beta$  depicts the probability of accepting  $H_0$  inspite of differences at the 95% confidence level.

Period	$b_{\text{geod}} \pm \sigma$ [m w.e.]	$b_{\text{glac}} \pm \sigma$ [m w.e.]	$\Delta b$ [m w.e.]	$\sigma_{\text{comvar}}$ [m w.e.]	$\delta$ no unit	$H_0$ : 95 no unit	$\beta$ : 95 [%]
2001/2002	-0.685 ± 0.16	-0.624 ± 0.21	+0.061	0.26	0.24	yes	94
2002/2003	-2.713 ± 0.20	-1.796 ± 0.21	+0.917	0.29	3.21	no	11
2003/2004	-0.654 ± 0.09	-0.651 ± 0.21	+0.003	0.23	0.01	yes	95
2004/2005	-1.028 ± 0.17	-1.022 ± 0.21	+0.006	0.27	0.02	yes	95
2005/2006	-2.091 ± 0.19	-1.493 ± 0.21	+0.598	0.28	2.11	no	44
2006/2007	-1.363 ± 0.10	-1.813 ± 0.21	-0.450	0.23	-1.97	no	50
2007/2008	-1.252 ± 0.11	-1.246 ± 0.21	+0.006	0.23	0.03	yes	95
2008/2009	-1.209 ± 0.10	-1.182 ± 0.21	+0.027	0.23	0.12	yes	95
2009/2010	-0.798 ± 0.09	-0.792 ± 0.21	+0.006	0.22	0.03	yes	95
2010/2011	-1.249 ± 0.07	-1.423 ± 0.21	-0.174	0.22	-0.79	yes	88
01/11	-12.45 ± 0.20	-12.04 ± 0.65	+0.41	0.29	1.44	yes	70
01-11cum	-12.99 ± 0.78	-12.04 ± 0.65	+0.95	0.81	1.18	yes	78

740